Supplementary Material (ESI) for Analyst
This journal is (C) The Royal Society of Chemistry 2007

Electrical Detection of *Hepatitis C* Virus RNA on Single Wall Carbon Nanotube-Field Effect Transistors

Tawab Dastagir,[a] Erica S. Forzani,[a] Ruth Zhang,[b] Islamshah Amlani,[b] Larry A. Nagahara,[b] Raymond Tsui[b] and Nongjian Tao[*a]

a Department of Electrical Engineering, Arizona Institute for Nano-electronics, Arizona State University, Tempe, AZ 85282-5706, USA.
b Embedded Systems Research Center, Motorola Labs, Tempe, AZ 85284-1806 USA.
** E-mail: nongjian.tao@asu.edu, Fax: 480-965-8118, Tel: 480-965-4456.*

Electronic Supplementary Information:

Fabrication of SWNT devices. The SWNT-FET devices used here were fabricated using a chemical vapor deposition (CVD) technique catalyzed by a thin Al/Ni stack. The catalysts were deposited on a heavily doped Si wafer with a 200 nm oxide layer. An array of gold electrodes (~ 300 nm thick) separated by μm-sized gaps and aligned to overlap the catalyst pads was thermally evaporated. The devices were annealed (~600 °C) in a hydrogen-rich environment to ensure better contact between the nanotubes and the metallic electrodes. The catalyst island density and pattern controlled the density of carbon nanotubes grown. Higher density of catalyst seeds allowed multiple SWNTs to be obtained in a single gap (Fig. 1a). We used low and high density SWNT devices. Low density SWNT devices consisted of few (1 to 4) SWNTs between a pair of gold electrodes (1-2 um gap, 2-um width, 250-nm thick) while high density devices comprised multiple SWNTs bridging interdigitated electrodes (finger width: 1.5 um) with gap from 1 to 10 um.

Electrochemical breaking down of metallic tubes. Before starting the SWNT modification, we characterized each device by measuring the I_d–V_g properties at various gate voltages applied to the back of the chips. The characterization showed pure p-type semiconducting, pure metallic and mixed p-type/metallic devices. Devices with pure p-type features were used in our experiments. In the case of mixed p-type/metallic devices we broke down the metallic tubes as many as possible to get pure p-type semiconducting devices. Many approaches has been used for breaking down carbon nanotubes.[1, 2] We used over-oxidation potentials to destroy the metallic tubes while p-type behavior tubes are turned off through the gate potential. Carbon nanotubes have strong carbon-carbon bonds able to withstand very high current densities, exceeding 10^9 A/cm^2.[1, 2] However, at high enough currents, nanotubes ultimately fail due to the rapid oxidation of the carbon shell. Our approach used a combination of fixed electrochemical gate potential (V_g) and a variable bias potential (V_b). Electrochemical gate potential was fixed to -0.2 V vs Ag/AgCl at WE1 to turn off the p-type tubes of our devices. High potential was then applied at WE2. A V_b swept from 0.5 to 1.5V in phosphate buffer solution (PBS) with pH > 7 was applied to induce carbon oxidation. Fig. 1b shows the I_d-V_g curves before and after the breakdown. Before and after breakdown, the I_{on}/I_{off} ratio value was ~3 and ~14, respectively. In general, I_{on}/I_{off} values resulting from breaking down were variable and depended on the gap size between gold electrodes. Better I_{on}/I_{off} ratio was found on devices with larger gap size.

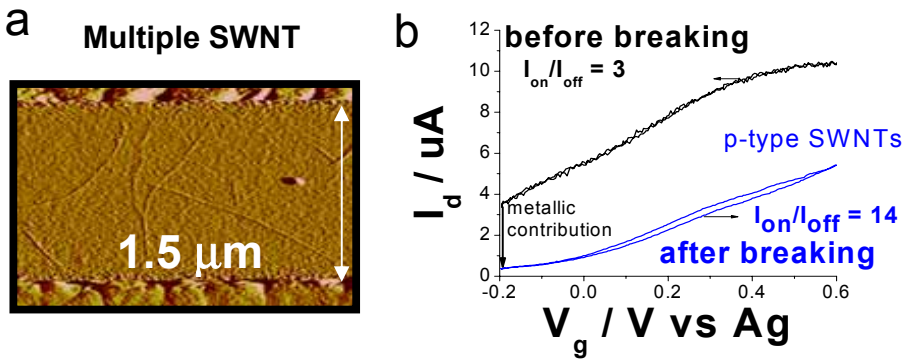

Fig. 1. (a) AFM images of devices with high densitiy of SWNTs between interdigitated electrodes. (b) I_d-V_g curves obtained on a multiple SWNT device in PBS pH = 7.4 before and after electrochemical breaking down of metallic tubes. V_b = -10 mV.

Conductance behavior of PNA-modified SWNT devices. Fig. 2a-b show the I_d-V_g curves before and after PNA adsorption on bare SWNT-FET device in buffer and DI, respectively. The curves marked as "before" shows the p-type behavior of bare SWNT devices. According to IUPAC electrochemical sign convention, p-type behavior of the SWNT devices was defined by increasing drain current values with increasing electrochemical gate positive potentials values. So, for the convention used in this communication, more positive V_g values increase the concentration of positively charged holes (p-type carriers). As it is stated in the communication, incubation of the device with PNA capture probe on the device resulted, with equal probability, either in a decrease in the transconductance, $g_m = (\partial I_d/\partial V_g)|_{Vb=10\ mV}$, or in a decrease of g_m associated with a small positive shift in threshold potential (V_{th}) (Fig. 2a-b). Since p-type conductance features obtained in water were similar to those found in buffer it is likely that impurities (in water or from the chip) as well as dissolution of CO_2 from air, which renders an equilibrium pH ~ 5.5, were responsible for ionic conduction and provided enough ionic strength in solution to allow electrochemical gate control. A possible source of the decrease of g_m could be a change of the capacitance due to the PNA adsorption on SWNT wall, SWNT/Au contacts or on gold electrodes. To rule out the last two possibilities, which would preclude the use of a SWNT-FET for channel conductance sensing applications, we performed backgate conductance measurements (I_d-V_{bg} curves) in air on contact passivated devices where the applied gate voltage is not affected by the area of the electrodes (Fig. 2c). We found that the I_d-V_{bg} curves obtained after PNA adsorption showed similar changes to those observed in the I_d-V_g (electrochemical gate potential) curves, suggesting a g_m change induced by PNA adsorption on SWNT walls.

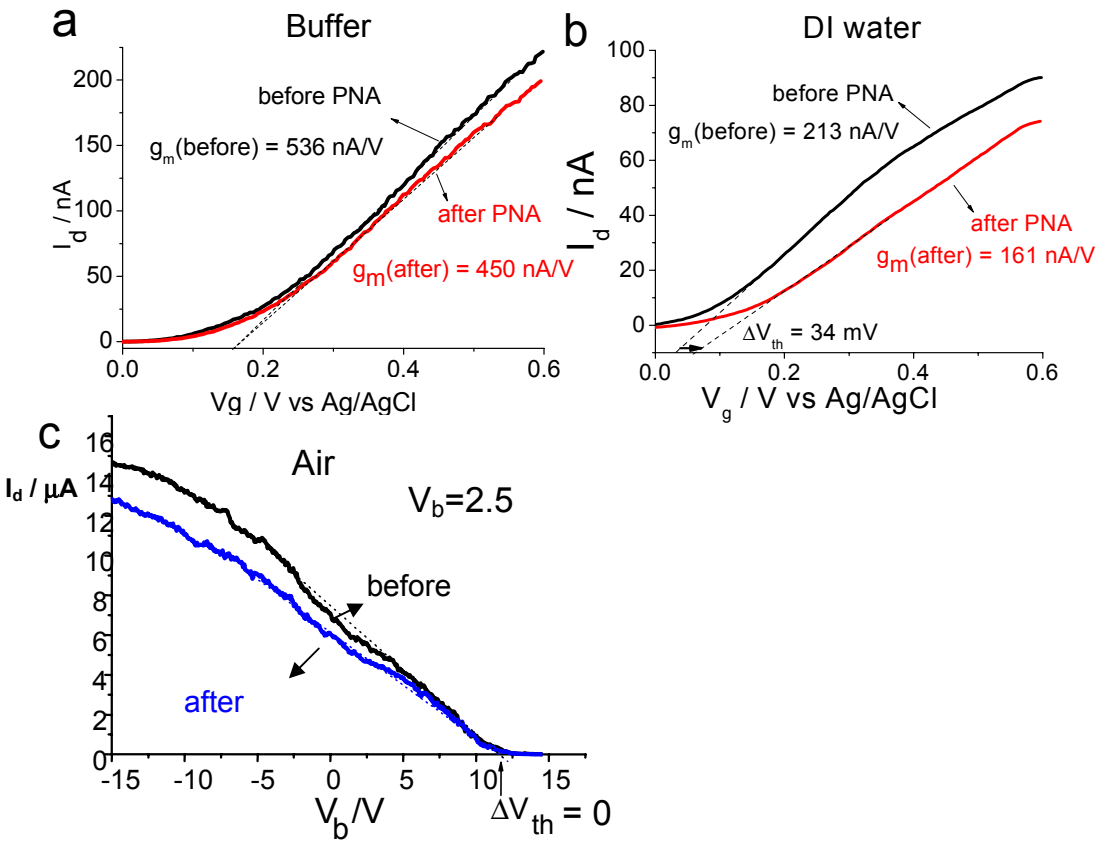

Fig. 2. p-type branches of I_d vs electrochemical (V_g) and backgate (V_{bg}) potential before and after PNA adsorption on SWNT-FET device in: buffer (a), DI water (b), air (c). (a and c) g_m decrease after PNA adsorption without changing threshold voltage (V_{th}). (b) Both V_{th} and g_m change after PNA adsorption. Forward and backward currents were averaged.

Estimation of PNA surface coverage on SWNT devices. We explored the possibility of estimating PNA surface coverage (θ_{PNA}) by assuming capacitance changes due to PNA adsorption taken place only on SWNT walls. To simplify, we considered only those cases with pure g_m changes. Under these conditions and far from saturation I_d, the electrochemically-gated transconductance for bare (g_m(bare)) and PNA-modified (g_m(PNA)) SWNT can be expressed as:[3]

$$g_m(\text{bare}) = \mu C_g' V_d / L \quad (1)$$
$$g_m(\text{PNA}) = \mu C_g'(\text{PNA}) V_d / L \quad (2)$$

where μ is the mobility of SWNT, V_d is source-drain voltage, L is the length of SWNT, C_g' is the capacitance of a bare SWNT determined by quantum capacitance (C_q) and liquid gate capacitance (C_{lg}) in series:[4]

$$1/C_g' = 1/C_q + 1/C_{lg} \quad (3)$$

and C_g'(PNA) is the capacitance after PNA adsorption with contributions from C_q in series with two capacitors C_{lg} and PNA capacitance (C_{PNA}) in parallel according to:

$$1 / C_g'(\text{PNA}) = 1/C_q + 1/ [\theta_{PNA} C_{PNA} + (1-\theta_{PNA}) C_{lg}] \quad (4)$$

The values of each capacitance component were estimated as follows:

- C_{lg} from $\varepsilon_o \kappa A_{SWNT} / \lambda_D$ where εo is permittivity of free space, κ is the dielectric constant of the liquid (80 for buffer), A_{SWNT} is the area of the SWNT ($2 \pi r L$, L = 1 or 1.5 μm and r= 1 nm) and λ_D is the Debye length (2.6 nm for buffer solution of ionic strength of 14 mM). The resulting value is 1.7×10^{-9} F/(m × tube).

- C_q from literature data 4×10^{-10} F/(m × tube).[5]

- C_{PNA} from $\varepsilon_o \kappa_{org} A_{SWNT} / d_{PNA}$ where κ_{org} is the dielectric constant of an organic layer (assumed ~ 3 for PNA), d_{PNA} is the averaged thickness of a PNA layer (1 nm). The estimated C_{PNA} value is 1.67×10^{-10} F/(m × tube). For 4 SWNT of 1.5-μm length, a value of $\sim 1 \times 10^{-15}$ F is assessed.

The C_g'(PNA) value was obtained from eqs.(1)-(2):

$$C_g'(PNA) = [g_m(PNA)/ g_m(bare)] \times C_g' (bare) \qquad (5)$$

using experimental values of g_m(bare) and g_m(PNA) as well as the estimated C_g'(bare) from eq.(3). The C_g'(bare) values used in the calculation of C_g'(PNA) were validated by comparing mobility values of bare SWNT (1000 cm^2/V-s in buffer) calculated from eq.(1) which were of same order of those obtained from backgate experiments (~4000 cm^2/V-s) using geometric dimensions of the FET. The agreement between these values assessed from different ways indicates that reasonable values of C_{lg} and C_q were used for C_g'(PNA) calculation. The assessed mobilities were within the range of those reported previously CVD-grown SWNTs.[5] C_g'(PNA) values in the range of ~1.1 x 10^{-15} F in buffer were obtained and θ_{PNA} values of 0.8-0.9 were estimated from eq.(4). This surface coverage indicates that a high percentage of the SWNT area is covered by PNA. It also indicates that we could effectively adsorb PNA in the sidewall of the SWNTs using our experimental procedure.

Determination of PNA-RNA_{com} affinity constant. The affinity constant of PNA –RNA_{com} was assessed by High Resolution Differential-Surface Plasmon Resonance (HRD-SPR) (Fig. 3). Differential SPR Angle changes between a sensing area modified with covalently attached PNA + Bovine Serum Albumin (BSA) and a reference area modified with BSA were monitored upon increasing concentrations of RNA_{com} and accounted for RNA_{com} –PNA hybridization. Quasi-stationary responses of SPR signal stabilized after solution stirring were obtained as a function of RNA_{com} concentration and the PNA-RNA_{com} affinity constant was estimated from fitting to Langmuir equation. A value of $K_{aff} = (3 \pm 1) \times 10^{10}$ M^{-1} was obtained.

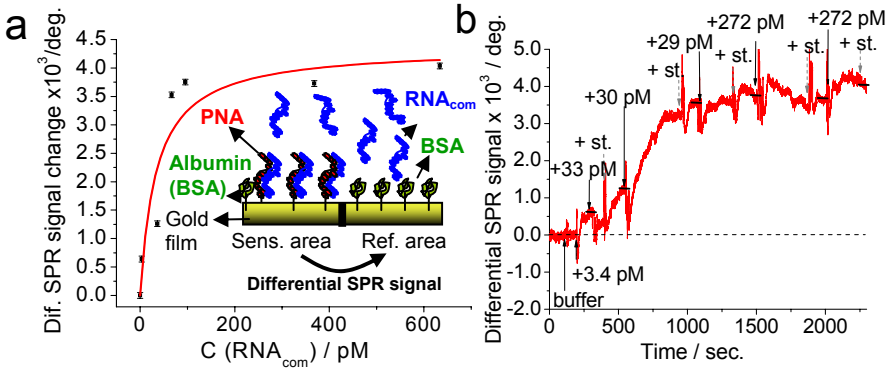

Fig. 3. (a) Inset: Schematic representation of the HRD-SPR sensor used to measure the affinity constant of PNA-RNA_{com} hybrids. PNA was covalently attached to the sensing area of the sensor while an inert layer of BSA was used to modified the reference area. The RNA_{com} binding on the sensing area was simultaneously measured with respect to the reference area to substract non-specific binding events on the sensor surface. (a)

SPR differential response vs RNA_{com} concentration (from b). Full line corresponds to a fitting of experimental results to Langmuir isotherm ($K_{aff} = (3 \pm 1) \times 10^{10}$ M^{-1}). (b) Real-time response of RNA_{com} binding on PNA-modified SPR sensor upon increasing RNA_{com} concentrations and stirring (+st.) steps. Tris buffer pH 7.4 (ionic strength = 14 mM).

Response of RNA_{com} on PNA-modified SWNT devices with Al_2O_3 passivated contacts. Interpretation about transduction mechanism of biomolecules detection on SWNT devices requires special care on controlling the nature of electronic contacts.[6, 7] For this reason, we study the incidence of different type of passivation on our SWNT- devices. We consistently found increasing transconductances (g_m) changes when RNA_{com} sequence was injected on PNA-modified SWNT devices previously passivated with dodecanethiol or with a microfabricated layer of Al_2O_3 on the contacts. Fig. 4 shows an example of the last case.

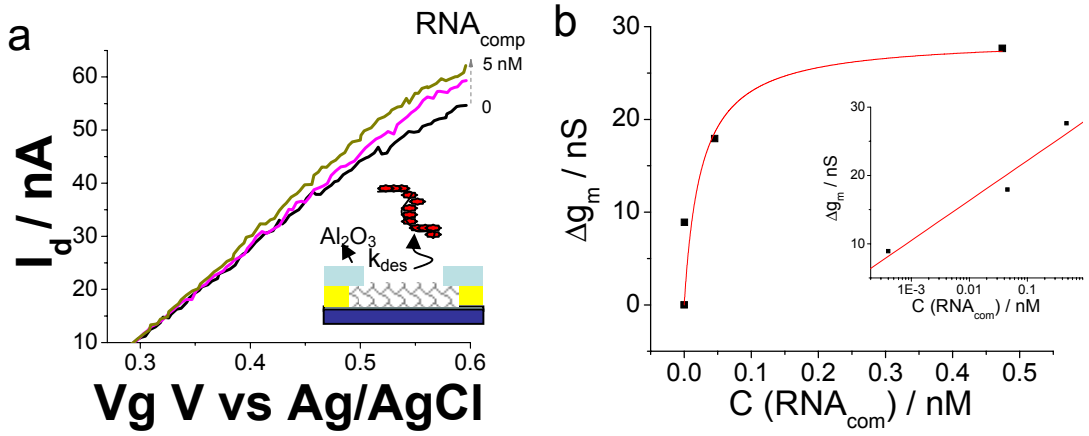

Fig. 4. (a) I_d-V_g curves resulting from exposure of a PNA modified SWNT-FET device towards increasing RNA_{com} concentrations. The device contacts were passivated with a microfabricated layer of Al_2O_3 (inset). (b) Calibration plots of g_m changes vs. RNA_{com} concentration. The full line shows the fitting with Langmuir isotherm ($K_{aff} = 2 \times 10^9$ M^{-1}).

References

(1) P. G. Collins, M. S. Arnold and P. Avouris, *Science,* 2001, **292**, 706.
(2) P. G. Collins, M. Hersam, M. S. Arnold, R. Martel and P. Avouris, *Phys. Rev. Lett.,* 2001, **86**, 3128.
(3) R. F. Pierret, *Field Effect Devices from Modular Series on Solid State Devices,* 1983, IV, Addisom-Wesley Publishing Co., Reading, Massachusetts.
(4) K. Besteman, J. O. Lee, F. G. M. Wiertz, H. A. Heering, C. Dekker and, *Nano Lett.,* 2003, **3**, 727.
(5) S. Rosenblatt, Y. Yaish, J. Park, J. Gore, V. Sazonova and P. L. McEuen, *Nano Lett.,* 2002, **2**, 869.
(6) X. W. Tang, S. Bansaruntip, N. Nakayama, E. Yenilmez, Y. L. Chang and Q. Wang, *Nano Lett.,* 2006, **6**, 1632-1636.
(7) R. J. Chen, H. C. Choi, S. Bangsaruntip, E. Yenilmez, X. W. Tang, Q. Wang, Y. L. Chang, H. Dai and, *J Am. Chem. Soc.,* 2004, **126**, 1563.